

This article was downloaded by: [Anderle, Milan]

On: 23 July 2010

Access details: Access Details: [subscription number 924718943]

Publisher Taylor & Francis

Informa Ltd Registered in England and Wales Registered Number: 1072954 Registered office: Mortimer House, 37-41 Mortimer Street, London W1T 3JH, UK



## International Journal of Control

Publication details, including instructions for authors and subscription information:

<http://www.informaworld.com/smpp/title~content=t713393989>

### Advanced LMI based analysis and design for Acrobot walking

Milan Anderle<sup>ab</sup>; Sergej Čelikovský<sup>ab</sup>; Didier Henrion<sup>ac</sup>; Jiří Zikmund<sup>b</sup>

<sup>a</sup> Faculty of Electrical Engineering, Department of Control Engineering, Czech Technical University in Prague, 166 27 Prague, Czech Republic <sup>b</sup> Institute of Information Theory and Automation, Academy of Sciences of the Czech Republic, 182 08 Prague, Czech Republic <sup>c</sup> LAAS-CNRS, University of Toulouse, 31077 Toulouse, France

First published on: 24 June 2010

**To cite this Article** Anderle, Milan , Čelikovský, Sergej , Henrion, Didier and Zikmund, Jiří(2010) 'Advanced LMI based analysis and design for Acrobot walking', International Journal of Control, 83: 8, 1641 — 1652, First published on: 24 June 2010 (iFirst)

**To link to this Article:** DOI: 10.1080/00207179.2010.484468

**URL:** <http://dx.doi.org/10.1080/00207179.2010.484468>

PLEASE SCROLL DOWN FOR ARTICLE

Full terms and conditions of use: <http://www.informaworld.com/terms-and-conditions-of-access.pdf>

This article may be used for research, teaching and private study purposes. Any substantial or systematic reproduction, re-distribution, re-selling, loan or sub-licensing, systematic supply or distribution in any form to anyone is expressly forbidden.

The publisher does not give any warranty express or implied or make any representation that the contents will be complete or accurate or up to date. The accuracy of any instructions, formulae and drug doses should be independently verified with primary sources. The publisher shall not be liable for any loss, actions, claims, proceedings, demand or costs or damages whatsoever or howsoever caused arising directly or indirectly in connection with or arising out of the use of this material.

## Advanced LMI based analysis and design for Acrobot walking

Milan Anderle<sup>ab\*</sup>, Sergej Čelikovský<sup>ab</sup>, Didier Henrion<sup>ac</sup> and Jiří Zikmund<sup>b</sup>

<sup>a</sup>Faculty of Electrical Engineering, Department of Control Engineering, Czech Technical University in Prague, Technická 2, 166 27 Prague, Czech Republic; <sup>b</sup>Institute of Information Theory and Automation, Academy of Sciences of the Czech Republic, Pod Vodárenskou věží 4, 182 08 Prague, Czech Republic; <sup>c</sup>LAAS-CNRS, University of Toulouse, 7 avenue du colonel Roche, 31077 Toulouse, France

(Received 11 December 2009; final version received 7 April 2010)

This article aims to further improve previously developed design for Acrobot walking based on partial exact feedback linearisation of order 3. Namely, such an exact system transformation leads to an almost linear system where error dynamics along trajectory to be tracked is a 4-dimensional linear time-varying system having three time-varying entries only, the remaining entries being either zero or one. In such a way, exponentially stable tracking can be obtained by quadratically stabilising a linear system with polytopic uncertainty. The current improvement is based on applying linear matrix inequalities (LMI) methods to solve this problem numerically. This careful analysis significantly improves previously known approaches. Numerical simulations of Acrobot walking based on the above-mentioned LMI design are demonstrated as well.

**Keywords:** linear matrix inequalities; underactuated mechanical systems; walking robots

### 1. Introduction

Efficient control of underactuated mechanical systems constitutes one of the most challenging problems of recent decades, see Fantoni and Lozano (2002), Zikmund and Moog (2006) and references therein. Reliable and economic walking is a typical example of studies involving both control and robotic communities. One of the simplest underactuated mechanical systems is the Acrobot. Despite being a seemingly simple system, the Acrobot comprises many important features of underactuated walking robots having degree of underactuation equal to one. Following ideas of Spong (1998) and Grizzle, Moog, and Chevallereau (2005) one can show that any  $n$ -link having  $n-1$  actuators between its links can be decomposed into a fully actuated system and an Acrobot-like underactuated system ‘disturbed’ by some variables from that fully actuated (and therefore fully exact feedback linearisable) subsystem. In other words, control strategies developed for Acrobot only could be actually straightforwardly generalised to the case of any  $n$ -link having  $n-1$  actuators between its links. As a consequence, effective control of the Acrobot is an important step on the route to underactuated walking. Recently, numerous papers have addressed stabilisation of its inverted position, extending its domain of attraction (Hauser and Murray 1990; Furuta, Yamakita, and Kobayashi 1991; Bortoff and

Spong 1992; Wiklund, Kristenson, and Åström 1993), or even stable walking-like movement (Čelikovský and Zikmund 2007; Zikmund, Čelikovský, and Moog 2007; Čelikovský, Zikmund, and Moog 2008).

This article is a continuation of the research initiated in Čelikovský and Zikmund (2007), Zikmund et al. (2007), Čelikovský et al. (2008). In Čelikovský et al. (2008), the asymptotical tracking of a suitable target trajectory generated by an open-loop reference control was obtained. As might have been expected, asymptotical tracking constitutes a principally more complicated problem than stabilisation since the corresponding error dynamics has a more complex structure than the Acrobot model itself. In particular, designed tracking feedback could handle limited initial tracking error only and its performance was limited to the case when the Acrobot walking-like movement was very slow. This was caused by a specific analytic method to stabilise tracking error dynamics. Despite removing the key drawback of slow velocity in the analytical design in Anderle and Čelikovský (2009) using special transformation of the error dynamics, the resulting feedback still imposes unrealistically high torques. Therefore, a natural idea is to involve more precise, though numerical only, design based on linear matrix inequalities (LMI) optimisation of the feedback gains to significantly improve previous limited results. Recently, the first attempt to involve numerical LMI

\*Corresponding author. Email: anderle@utia.cas.cz

based approach was made in Anderle, Čelikovský, Henrion, and Zikmund (2009). Nevertheless, results presented there use quite rough polytopic estimates for tracked walking-like trajectory which results into unrealistically high control efforts.

The purpose of this article is to improve these results using two strategies. First, tighter polytopic estimates of the tracked trajectory may be used. Secondly, additional criterion for LMI optimisation can be imposed that would directly or indirectly impose limits on the level of the control action. As will be shown in the sequel, these strategies are successful and significantly improve the results of Anderle et al. (2009) and Anderle and Čelikovský (2009).

The rest of the article is organised as follows. The next section briefly presents the model of the Acrobot together with the main theoretical prerequisites necessary for further problem analysis. Section 3 describes the essence of the LMI approach while numerical optimisation results and subsequent simulations of Acrobot walking are presented in Section 4. The final section draws briefly some conclusions and discusses some open future research outlooks towards efficient underactuated walking.

## 2. Acrobot

The Acrobot depicted in Figure 1 is a special case of an  $n$ -link chain with  $n - 1$  actuators attached by one of its ends to a pivot point through an unactuated rotary joint. Such a system can be modelled by the usual Lagrangian approach, see Greiner (2003). The corresponding Lagrangian is as follows:

$$\mathcal{L}(q, \dot{q}) = K - V = \frac{1}{2} \dot{q}^T D(q) \dot{q} - V(q), \quad (1)$$

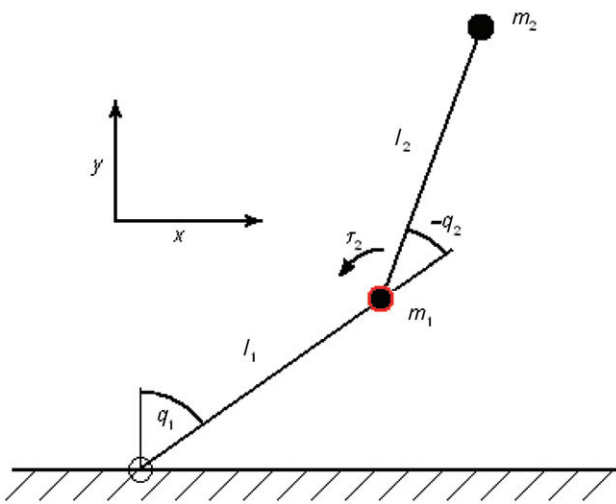


Figure 1. Acrobot.

where  $q$  denotes an  $n$ -dimensional vector on the configuration manifold  $Q$  and  $D(q)$  is the inertia matrix,  $K$  is the kinetic energy and  $V$  is the potential energy of the system. The resulting Euler–Lagrange equation is

$$\begin{bmatrix} \frac{d}{dt} \frac{\partial \mathcal{L}}{\partial \dot{q}_1} - \frac{\partial \mathcal{L}}{\partial q_1} \\ \frac{d}{dt} \frac{\partial \mathcal{L}}{\partial \dot{q}_2} - \frac{\partial \mathcal{L}}{\partial q_2} \\ \vdots \\ \frac{d}{dt} \frac{\partial \mathcal{L}}{\partial \dot{q}_n} - \frac{\partial \mathcal{L}}{\partial q_n} \end{bmatrix} = \begin{bmatrix} 0 \\ \tau_2 \\ \vdots \\ \tau_n \end{bmatrix} = \bar{u}, \quad (2)$$

where  $\bar{u}$  stands for the vector of external controlled forces. System (2) is a so-called *underactuated* mechanical system having degree of underactuation equal to one, see Spong (1998). Moreover, the underactuated angle is at the pivot point. Equation (2) leads to a dynamic equation of the form

$$D(q)\ddot{q} + C(q, \dot{q})\dot{q} + G(q) = \bar{u}, \quad (3)$$

where  $D(q)$  is the inertia matrix,  $C(q, \dot{q})$  contains Coriolis and centrifugal terms,  $G(q)$  contains gravity terms and  $\bar{u}$  stands for the vector of external forces.

For the Acrobot, these computations lead to a second-order non-holonomic constraint and a kinetic symmetry, i.e. the inertia matrix depends only on the second variable  $q_2$ :

$$D(q) = \begin{bmatrix} \theta_1 + \theta_2 + 2\theta_3 \cos q_2 & \theta_2 + \theta_3 \cos q_2 \\ \theta_2 + \theta_3 \cos q_2 & \theta_2 \end{bmatrix}, \quad (4)$$

and the other systems matrices are given by

$$C(q, \dot{q}) = \begin{bmatrix} -\theta_3 \sin q_2 \dot{q}_2 & -(\dot{q}_2 + \dot{q}_1)\theta_3 \sin q_2 \\ \theta_3 \sin q_2 \dot{q}_1 & 0 \end{bmatrix}, \quad (5)$$

$$G(q) = \begin{bmatrix} -\theta_4 g \sin q_1 - \theta_5 g \sin(q_1 + q_2) \\ -\theta_5 g \sin(q_1 + q_2) \end{bmatrix}, \quad (6)$$

where the 2-dimensional configuration vector  $(q_1, q_2)$  consists of angles defined on Figure 1 and

$$\begin{aligned} \theta_1 &= (m_1 + m_2)l_1^2 + I_1, & \theta_2 &= m_2 l_2^2 + I_2, \\ \theta_3 &= m_2 l_1 l_2, & \theta_4 &= (m_1 + m_2)l_1, & \theta_5 &= m_2 l_2. \end{aligned} \quad (7)$$

The *partial exact feedback linearisation* method is based on a system transformation into a new system of coordinates that display linear dependence between an output and a new input, see Isidori (1996). From a theoretical point of view, the mechanical system dynamics is described by an  $n$ -dimensional state-space equation. Static state-feedback linearisation using a suitable output function of relative degree  $r$  yields a linear subsystem of dimension  $r$ . In other words,

the maximal feedback linearisation problem consists in finding a linearising function with maximal relative degree. In Grizzle et al. (2005) it was shown that if the generalised momentum conjugate to the cyclic variable is not conserved (as it is the case of the Acrobot) then there exists a set of outputs that defines one-dimensional exponentially stable zero dynamics. In the case of the Acrobot it means that it is possible to find a function  $\bar{y}(q, \dot{q})$  with relative degree 3 that transforms the original system (3) by a local coordinate transformation  $z = T(q, \dot{q})$ , namely

$$z_1 = \bar{y}, \quad z_2 = \dot{\bar{y}}, \quad z_3 = \ddot{\bar{y}}, \quad z_4 = f(q, \dot{q}), \quad (8)$$

into a new input/output linear system with one-dimensional nonlinear zero dynamics:

$$\begin{aligned} \dot{z}_1 &= z_2, \quad \dot{z}_2 = z_3, \quad \dot{z}_3 = \alpha(q, \dot{q})\tau_2 + \beta(q, \dot{q}) = w, \\ \dot{z}_4 &= \psi_1(q, \dot{q}) + \psi_2(q, \dot{q})\tau_2. \end{aligned} \quad (9)$$

In the case of the Acrobot there are two independent functions with relative degree 3 transforming the system into the desired form<sup>1</sup> (9), namely

$$\sigma = \frac{\partial \mathcal{L}}{\partial \dot{q}_1} = (\theta_1 + \theta_2 + 2\theta_3 \cos q_2)\dot{q}_1 + (\theta_2 + \theta_3 \cos q_2)\dot{q}_2, \quad (10)$$

$$\begin{aligned} p &= q_1 + \frac{q_2}{2} \\ &+ \frac{2\theta_2 - \theta_1 - \theta_2}{\sqrt{(\theta_1 + \theta_2)^2 - 4\theta_3^2}} \arctan\left(\sqrt{\frac{\theta_1 + \theta_2 - 2\theta_3}{\theta_1 + \theta_2 + 2\theta_3}} \tan \frac{q_2}{2}\right). \end{aligned} \quad (11)$$

The zero dynamics is used to investigate internal stability when the corresponding output is forced to zero. For the simplest cases  $\bar{y} = Cp$  or  $\bar{y} = C\sigma$  the resulting zero dynamics is only critically stable. However, considering the output function  $\bar{y} = C_1p(q) + C_2\sigma(q, \dot{q})$  one gets the following zero dynamics  $\dot{p} + C_1[C_2d_{11}(q_2)]^{-1}p = 0$  which is asymptotically stable whenever  $C_1/C_2$  is positive,  $d_{11}(q_2)$  being the corresponding part of the inertia matrix  $D$  in (3). Unfortunately, the corresponding transformations have a complex set of singularities, unless  $C_1$  is very small, which is not suitable for practical purposes.

In Čelikovský et al. (2008), it was shown that the above functions  $p, \sigma$  having maximal relative degree 3 can be used in a slightly different way. Namely, the following transformation can be defined:

$$\xi_1 = p, \quad \xi_2 = \sigma, \quad \xi_3 = \dot{\sigma}, \quad \xi_4 = \ddot{\sigma}. \quad (12)$$

Notice that by (10), (11) and some straightforward but laborious computations the following relation holds:

$$\dot{p} = d_{11}(q_2)^{-1}\sigma, \quad (13)$$

where  $d_{11}(q_2) = (\theta_1 + \theta_2 + 2\theta_3 \cos q_2)$  is the corresponding element of the inertia matrix  $D$  in (3). Applying (12), (13) to (3) we obtain Acrobot dynamics in partial exact linearised form

$$\begin{aligned} \dot{\xi}_1 &= d_{11}(q_2)^{-1}\xi_2, \quad \dot{\xi}_2 = \xi_3, \quad \dot{\xi}_3 = \xi_4, \\ \dot{\xi}_4 &= \alpha(q)\tau_2 + \beta(q, \dot{q}) = w, \end{aligned} \quad (14)$$

with new coordinates  $\xi$  and input  $w$  being well defined whenever  $\alpha(q)^{-1} \neq 0$ . An important feature here is that the set of possible singularities where  $\alpha(q)^{-1} = 0$  depends only on positions, not on velocities, and it has favourable properties, as will be shown in detail later.

To determine the region where such a transformation can be applied, let us express it explicitly. Namely, straightforward computations show that

$$\xi = \begin{bmatrix} \xi_1 \\ \xi_2 \\ \xi_3 \\ \xi_4 \end{bmatrix} = T(q_1, q_2, \dot{q}_1, \dot{q}_2) := \begin{bmatrix} T_1 \\ T_2 \\ T_3 \\ T_4 \end{bmatrix}, \quad (15)$$

$$\begin{bmatrix} T_1 \\ T_3 \\ T_2 \\ T_4 \end{bmatrix} = \begin{bmatrix} p(q_1, q_2) \\ \theta_4 g \sin q_1 + \theta_5 g \sin(q_1 + q_2) \\ \Phi_2(q_1, q_2) \begin{bmatrix} \dot{q}_1 \\ \dot{q}_2 \end{bmatrix} \end{bmatrix}, \quad (16)$$

where  $p, \sigma$  are given by (10,11) and  $\Phi_2$  by (21) later on. Further, denote

$$\phi = \begin{bmatrix} \phi_1(\xi_1, \xi_3) \\ \phi_2(\xi_1, \xi_3) \end{bmatrix}, \quad (17)$$

such that

$$T_1(\phi_1(\xi_1, \xi_3), \phi_2(\xi_1, \xi_3)) = \xi_1, \quad T_3(\phi_1(\xi_1, \xi_3), \phi_2(\xi_1, \xi_3)) = \xi_3. \quad (18)$$

It holds by (15)–(16) that

$$\frac{\partial [\xi_1, \xi_3, \xi_2, \xi_4]^T}{\partial [q^T, \dot{q}^T]^T} = \begin{bmatrix} \Phi_1(q_1, q_2) & 0 \\ \Phi_3(q, \dot{q}) & \Phi_2(q_1, q_2) \end{bmatrix}, \quad (19)$$

where  $q := [q_1, q_2]^T$ ,  $\Phi_3(q, \dot{q})$  is a certain  $(2 \times 2)$  matrix of smooth functions while

$$\begin{aligned} \Phi_1(q_1, q_2) &= \begin{bmatrix} 1 & \frac{\theta_2 + \theta_3 \cos q_2}{\theta_1 + \theta_2 + 2\theta_3 \cos q_2} \\ \theta_4 g \cos q_1 + \theta_5 g \cos(q_1 + q_2) & \theta_5 g \cos(q_1 + q_2) \end{bmatrix}, \end{aligned} \quad (20)$$

$$\begin{aligned} \Phi_2(q_1, q_2) &= \begin{bmatrix} \theta_1 + \theta_2 + 2\theta_3 \cos q_2 & \theta_2 + \theta_3 \cos q_2 \\ \theta_4 g \cos q_1 + \theta_5 g \cos(q_1 + q_2) & \theta_5 g \cos(q_1 + q_2) \end{bmatrix}. \end{aligned} \quad (21)$$

Further, it obviously holds for (17), (18) that

$$\begin{aligned} & \frac{\partial \phi(\xi_1, \xi_3)}{\partial [\xi_1, \xi_3]^T} \\ &= \Phi_1^{-1}(q_1, q_2) \\ &= \frac{1}{s(q)} \begin{bmatrix} \theta_5 g \cos(q_1 + q_2) & \frac{-\theta_2 - \theta_3 \cos q_2}{\theta_1 + \theta_2 + 2\theta_3 \cos q_2} \\ \left\{ \begin{array}{c} -\theta_4 g \cos q_1 \\ -\theta_5 g \cos(q_1 + q_2) \end{array} \right\} & 1 \end{bmatrix}, \end{aligned} \quad (22)$$

$$\begin{aligned} s(q) &:= \det \Phi_1 = \frac{\det \Phi_2}{d_{11}(q)} \\ &= g \frac{\left\{ \begin{array}{c} (\theta_1 + \theta_3 \cos q_2) \theta_5 \cos(q_1 + q_2) \\ -(\theta_2 + \theta_3 \cos q_2) \theta_4 \cos q_1 \end{array} \right\}}{d_{11}(q)}. \end{aligned} \quad (23)$$

Moreover, the coordinate change (15), (16) is locally invertible at each point where

$$s(q) \neq 0. \quad (24)$$

Indeed,  $D(q) > 0$  and the above  $\alpha(q, \dot{q})$ ,  $\beta(q, \dot{q})$  from (14) are given as

$$\alpha(q, \dot{q}) = \frac{\det \Phi_2}{\det D(q)}, \quad \begin{bmatrix} 0 \\ \beta(q, \dot{q}) \end{bmatrix} = \Phi_3(q, \dot{q}) \dot{q}, \quad (25)$$

where  $\Phi_2$  is given by (21). By virtue of Čelikovský (1994) and the references therein, the coordinate change (16) is globally invertible on any open set where (24) holds and which is both connected and simply connected. In other words, the Acrobot model is state and feedback equivalent to system (14) on any such set. Figure 2 depicts some of these sets. Moreover, for possible walking application, the following lemma is useful, see Čelikovský et al. (2008).

**Lemma 2.1:** *Relation (24) holds if the Acrobot centre of mass is strictly above the surface and*

$$\begin{aligned} (m_1 + m_2)l_1^2 + I_1 &> m_2 l_1 l_2, \\ m_2 l_2^2 + I_2 &> m_2 l_1 l_2, \\ q_1 \in (-\pi/2, \pi/2), \quad q_1 + q_2 &\in (3\pi/2, \pi/2). \end{aligned}$$

**Proof:** Instead of performing tedious computations, let us give the following mechanics motivated proof. First, notice that (24) means that matrix (21) is regular. Secondly, one can easily see that the first assumption of Lemma 2.1 is equivalent to  $\theta_1 > \theta_3$ ,  $\theta_2 > \theta_3$ , cf. (7), therefore the entries of the first row of matrix (21) are always strictly positive. At the same time, the first entry of the second row of matrix (21) is the overall Acrobot potential energy with respect to the ground surface while the second entry of the second row is the potential energy of the second link only with respect to

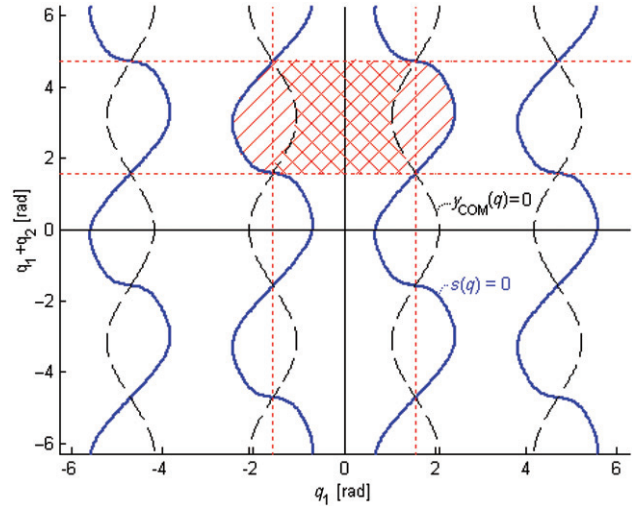


Figure 2. Singularities and possible regular set of coordinate change (16). Here  $s(q)$  is given by (23), while  $y_{COM}(q)$  stands for the vertical distance of the Acrobot centre of mass from the ground. Notice that in real application this distance should obviously be significantly bigger than zero.

the actuated joint position. Notice that  $q_1 \in (-\pi/2, \pi/2)$  means that the first link points upwards while  $q_1 + q_2 \in (3\pi/2, \pi/2)$  means that the second link points downwards. Therefore, the first entry of the second row of matrix (21) is positive, while its second entry is negative. Taking into account, as shown above, that the entries of the first row of the matrix (21) are strictly positive, one concludes that both rows of that matrix are always linearly independent, i.e. matrix (21) is regular and therefore  $s(q) \neq 0$ .  $\square$

**Remark 1:** Notice that the condition of Lemma 2.1 specifying that  $q_1 \in (-\pi/2, \pi/2)$  and  $q_1 + q_2 \in (3\pi/2, \pi/2)$  is quite natural in the case of walking-like movement of the Acrobot. Indeed, its violation means that either the stance leg is below or fully lying on the walking surface, or the swing leg points horizontally or upward. Apparently, such configurations are not likely or should be avoided during walking. Moreover, the remaining conditions of Lemma 2.1 obviously hold for almost any reasonable combination of lengths and masses, e.g. it holds for  $l_1 = l_2$  and, by continuity arguments, for sufficiently small  $|l_1 - l_2|$  as well. The last feature may be used to shorten slightly the swing leg during a step, to prevent hitting the ground. Again, walking robots having very different leg link lengths are unrealistic for many other practical reasons.

The situation is well demonstrated in Figure 2, where full lines show singularities  $s(q) = 0$  while dashed lines denote the configurations with centre of mass lying on the walking surface. Proof of Lemma 2.1 applies within the crosshatched area and any

reasonable walking takes place even deep inside this crosshatched area.

In the sequel we will therefore concentrate ourselves on the study of system (14). This system is almost linear, but there is a nonlinearity  $d_{11}(q_2)^{-1}$  in the first row that depends on  $q_2$  only. Instead of expressing this nonlinearity in coordinates  $\xi$  and trying to study its exact influence, one can use some favourable qualitative properties. Namely, one can easily see that

$$a_{\min} \leq d_{11}(q_2)^{-1} \leq a_{\max}, \quad (26)$$

with

$$a_{\min} = \frac{1}{m_2(l_1 + l_2)^2 + m_1 l_1^2 + I_1 + I_2}, \quad (27)$$

and

$$a_{\max} = \frac{1}{m_2(l_1 - l_2)^2 + m_1 l_1^2 + I_1 + I_2}. \quad (28)$$

Notice that the quantity

$$a_{\max} - a_{\min} = \frac{4l_1 l_2 m_2 (m_2(l_1 + l_2)^2 + m_1 l_1^2 + I_1 + I_2)^{-1}}{(m_2(l_1 - l_2)^2 + m_1 l_1^2 + I_1 + I_2)} \quad (29)$$

is quite small and therefore the nonlinearity  $d_{11}(q_2)^{-1}$  is actually varying in a quite narrow range. Therefore, its derivative also evolves in a favourable way, namely

$$\frac{\partial [d_{11}(q_2)^{-1}]}{\partial q_2} = (2\theta_3 \sin q_2) d_{11}(q_2)^{-2}, \quad (30)$$

$$\left| \frac{\partial [d_{11}^{-1}]}{\partial q_2} \right| \leq 2\theta_3 a_{\max}^2. \quad (31)$$

The above favourable properties of Acrobot partial linearisation will be used in the sequel for a feedback design ensuring exponentially tracking of a given walking-like trajectory.

Assume that an open-loop control generating a suitable single step reference trajectory is given on the time interval  $[0, T]$  in partial exact linearised coordinates (14). Therefore, our task is to track the following reference system

$$\dot{\xi}_1^{ref} = d_{11}^{-1}(q_2^{ref}) \xi_2^{ref}, \quad \dot{\xi}_2^{ref} = \xi_3^{ref}, \quad \dot{\xi}_3^{ref} = \xi_4^{ref}, \quad \dot{\xi}_4^{ref} = w^{ref}. \quad (32)$$

The following theorem gives a constructive and analytical way to asymptotically track reference system (32).

**Theorem 2.2:** Consider system (14) with the following feedback:

$$w = w^{ref} + \Theta^3 K_1 e_1 + \Theta^3 K_2 e_2 + \Theta^2 K_3 e_3 + \Theta K_4 e_4, \quad (33)$$

$$e =: \xi - \xi^{ref}.$$

Further, let  $K_1 < 0$  and  $K_{2,3,4}$  be such that the polynomial  $\lambda^3 + K_4 \lambda^2 + K_3 \lambda + K_2$  is Hurwitz. Then there exist  $\Theta > 0$ ,  $\mathcal{R} > 0$ ,  $\mathcal{B} > 0$  such that for all reference trajectories given by (32) and satisfying

$$\forall t \geq 0 \quad |s(\phi_2(\xi^{ref})(t))| \geq \mathcal{B} > 0, \quad (34)$$

$$|\xi_2^{ref}(t)| \leq \mathcal{R}, \quad \forall t \geq 0, \quad (35)$$

where  $\phi_2$  is given by (17), (18) and  $s(q)$  by (23). It follows that  $e(t) \rightarrow 0$  locally exponentially when  $t \rightarrow \infty$ .

The above theorem is proved in Čelikovský et al. (2008). It is based on a certain specific adaptation of high-gain technique, enabling to produce an exact mathematical proof of stability.

Notice the role of two positive constants defined by (34), (35). The first constant  $\mathcal{B}$  expresses how close the trajectory gets to singularity of the exact linearising transformation and does not constitute a serious drawback due to Lemma 2.1 and Remark 1. Nevertheless, small  $\mathcal{R}$  can be achieved only for slow walking velocity. Therefore, the main drawback of Theorem 2.2 is that the convergence is proved only for very slow walking speed. Moreover, this convergence is slow in simulations despite an unreasonable high torque at the actuated Acrobot joint.

Nevertheless, simulations show that the stabiliser works even for walking speeds significantly higher than those necessary for the theoretical proof. This indicates that the above drawbacks are caused by the analytical methods used for Theorem 2.2. Therefore, a natural idea is to try to stabilise the error dynamics using more sophisticated numerical methods.

To be more specific, let us repeat that during the proof of Theorem 2.2 in Čelikovský et al. (2008) it was shown that subtracting (32) from (14) one obtains

$$\dot{e}_1 = d_{11}^{-1}(\phi_2(\xi_1, \xi_3)) \xi_2 - d_{11}^{-1}(\phi_2(\xi_1^{ref}, \xi_3^{ref})) \xi_2^{ref}, \quad \dot{e}_2 = e_3, \quad \dot{e}_3 = e_4, \quad \dot{e}_4 = w.$$

Straightforward computations based on Taylor expansions give

$$\dot{e}_1 = \mu_2(t) e_2 + \mu_1(t) e_1 + \mu_3(t) e_3 + o(e), \quad (36)$$

$$\dot{e}_2 = e_3, \quad \dot{e}_3 = e_4, \quad (37)$$

$$\dot{e}_4 = w, \quad (38)$$

$$\mu_1(t) = \xi_2^{ref}(t) \frac{\partial [d_{11}^{-1}]}{\partial q_2} \frac{\partial \phi_2}{\partial \xi_1}(q_2^{ref}(t)), \quad (39)$$

$$\mu_2(t) = d_{11}^{-1}(q_2^{ref}(t)), \quad (40)$$

$$\mu_3(t) = \xi_2^{ref}(t) \frac{\partial [d_{11}^{-1}]}{\partial q_2} \frac{\partial \phi_2}{\partial \xi_3}(q_2^{ref}(t)), \quad (41)$$

$$q_2^{ref}(t) = \phi_2(\xi_1^{ref}(t), \xi_3^{ref}(t)), \quad q_2 \in [0, 2\pi). \quad (42)$$

In Čelikovský et al. (2008) it was shown that

$$|\mu_1(t)| \leq 2\theta_3 a_{\max}^2 (\theta_4 + \theta_5) \frac{\mathcal{R}}{\mathcal{B}}, \quad (43)$$

$$|\mu_3(t)| \leq 2\theta_3 a_{\max}^2 \frac{\mathcal{R}}{\mathcal{B}}, \quad 0 < a_{\min} \leq \mu_2(t) \leq a_{\max}, \quad (44)$$

where notation of Theorem 2.2 is used, in particular,  $\mathcal{R}$ ,  $\mathcal{B}$  are defined by (34), (35). Moreover, it turns out that for any given reference trajectory  $q^{ref}(t)$ , the functions  $\mu_{1,2,3}$  can be quite easily computed numerically using formulae (39), (40), (41). Summarising, one has to stabilise linear time-varying system using a linear feedback. One option is to use the quadratic stability concept that would ensure existence of a single linear feedback and a single quadratic Lyapunov function for all possible values of the three-dimensional parameter  $[\mu_1(t), \mu_2(t), \mu_3(t)]$ ,  $t \in [0, T]$  where  $T > 0$  is the time duration of a single step reference trajectory.

### 3. LMI based stabilisation of the error dynamics

It was shown at the end of the previous section that for reference trajectory tracking one has to solve the following stabilisation problem. Defining the state

$$x(t) = e(t)$$

as the error signal, consider the open-loop continuous time-varying linear system

$$\dot{x}(t) = A(t)x(t) + Bu(t),$$

$$A(t) = \begin{pmatrix} \mu_1(t) & \mu_2(t) & \mu_3(t) & 0 \\ 0 & 0 & 1 & 0 \\ 0 & 0 & 0 & 1 \\ 0 & 0 & 0 & 0 \end{pmatrix}, \quad B = \begin{pmatrix} 0 \\ 0 \\ 0 \\ 1 \end{pmatrix}. \quad (45)$$

The tracking problem consists in finding the state-feedback controller

$$u(t) = Kx(t), \quad K = [K_1 \ K_2 \ K_3 \ K_4], \quad (46)$$

producing the following closed-loop system:

$$\dot{x} = (A + BK)x = \begin{pmatrix} \mu_1(t) & \mu_2(t) & \mu_3(t) & 0 \\ 0 & 0 & 1 & 0 \\ 0 & 0 & 0 & 1 \\ K_1 & K_2 & K_3 & K_4 \end{pmatrix} x, \quad (47)$$

where bounds for  $\mu(t) = (\mu_1(t), \mu_2(t), \mu_3(t))$  are given by (43), (44).

Despite the entries of  $\mu(t)$  being *known* functions, the appealing idea is to treat them as *unknown disturbances* satisfying the above-mentioned given constraints. If constraints are tight enough, one can think about solving quadratic stability conditions and design a unique feedback stabilising such an ‘uncertain’ system. Obviously, such a feedback would be at the same time solving our tracking problem.

To pursue such an idea, let us obtain LMI conditions for quadratic stability. Let us recall here that quadratic stability is a particular case of robust stability, valid for arbitrarily fast time variation of the uncertain parameters, and certified by a unique quadratic-in-the-state parameter-independent Lyapunov function. Consider the well-known Lyapunov inequality to be solved for all values of  $\mu(t)$  by finding a suitable symmetric positive definite matrix  $S$  and a vector  $K$ :

$$(A(\mu) + BK)^T S + S(A(\mu) + BK) \leq 0, \quad (48)$$

$$S = S^T > 0. \quad (49)$$

Such a problem is in fact bilinear with respect to the unknowns. Denoting

$$Q = S^{-1}, \quad Y = KS^{-1}, \quad (50)$$

we derive the following LMI condition for quadratically stabilising feedback design:

$$A(\mu)Q + BY + (A(\mu)Q + BY)^T \leq 0, \quad Q > 0, \quad (51)$$

see e.g. Scherer and Weiland (2005, Section 5.2). Notice that pair  $(A(\mu), B)$  is controllable if and only if

$$\mu_1 \mu_3 + \mu_2 \neq 0. \quad (52)$$

Obviously, if the set of possible values of  $\mu$  contains, or stays close to, the singular set given by (52), LMI (51) becomes infeasible, or almost infeasible.

### 4. Numerical analysis and simulations

As already indicated, values of  $\mu(t)$  during a given single step can be computed numerically. In this section we provide a detailed account of approximate modelling of the  $\mu(t)$  trajectory, and corresponding LMI conditions used to generate a stabilising feedback gain.

To demonstrate our approach of tracking feedback design we use the so-called passive walking trajectory, developed in Čelikovský et al. (2008). Briefly, pseudo-passive walking trajectory is the one which is produced by zero virtual input  $w$ , i.e. by real torque  $\tau_2 = -\beta/\alpha$ , where  $\alpha$ ,  $\beta$  are given by (14). By physical considerations it means that the pseudo-passive trajectory maintains the constant speed of the centre of mass of the whole Acrobot. For such a trajectory,

the time-varying entries  $\mu_{1,2,3}(t)$  were computed numerically with high precision using the same Acrobot physical parameters as in Čelikovský et al. (2008). In the sequel, these entries will be embedded in various kinds of convex polytopic sets and the corresponding LMI problems solved, thereby obtaining quadratic stability of the error dynamics with various degrees of conservatism.

#### 4.1 Box

First, let us embed the trajectory into the following rectangular box (with edges parallel to the main axes), see Figure 3. Each vertex of the box is defined by a combination of upper and lower bounds on entries of  $\mu$ . Summarising, we have  $2^3 = 8$  LMI constraints

$$A_i Q + B Y + (A_i Q + B Y)^T \leq 0, \quad i = 1, \dots, 8 \quad (53)$$

modelled with the Matlab YALMIP parser and solved numerically with SeDuMi, giving the state-feedback gains matrix  $K = 10^5 \times (-1.9909 - 1.0082 - 0.10417 - 0.0020611)$  having Euclidean norm  $2.2341 \times 10^5$ . In the walking-like step trajectory simulations, the initial positions errors are zero but velocities errors are about 20%. The walking-like trajectory simulations in this paragraph are quite similar to those of Section 4.2, so they are not reproduced for conciseness. The main observation is that the torque used with the above high-gain feedback is too high to be realistic. More details on this rectangular box based design can be found in Anderle et al. (2009).

Summarising, the rectangular box-based design produces highly conservative and practically unacceptable design. This design can be combined with saturations significantly limiting torques to their realistic values, yet maintaining exponential tracking. Nevertheless, the last property can be checked only experimentally and the saturated torques principally and qualitatively differ from those non-saturated which makes almost unrealistic an analytical proof of saturated stability.

#### 4.2 Prism

Motivated by unrealistically high input torques in the previous section, an alternative design is considered here. To reduce the norm of the feedback gain, being the principal source of the high torques, we manually adjust the vertices of a polytope to fit closer the actual trajectory  $\mu(t)$ . The idea to construct such a tighter polytope is quite intuitive: a square with two vertices parallel to  $(\mu_1, \mu_3)$ -plane, centred at  $\mu(T/2)$ . The size of this square is tuned to imbed the trajectory into the polytope as tightly as possible.

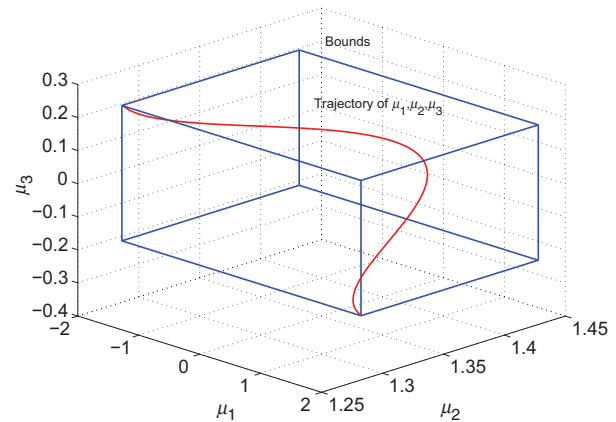


Figure 3. Trajectory  $\mu(t)$  embedded in a rectangular box.

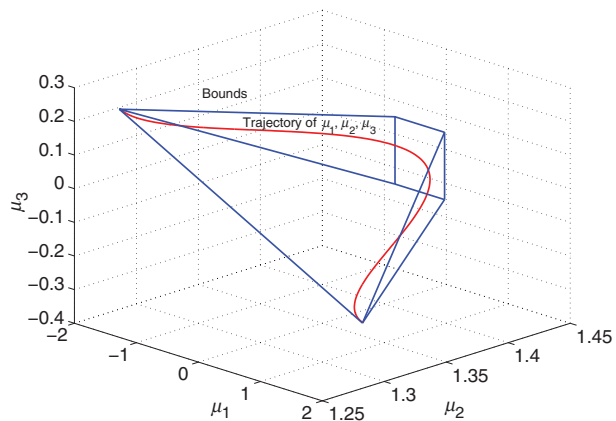


Figure 4. Trajectory  $\mu(t)$  and prismatic bounds.

When compared to the rectangular box modelling of the previous section, the number of LMI constraints is thereby reduced to six: two constraints are the same as previously, the remaining four constraints are defined via vertices relatively close to each other and centred around parameters value at the middle of the step. It is nicely seen from Figure 4 that this set is reasonably small and close to a tetrahedron. We will refer to this uncertainty model in the sequel as to the *prismatic bounds*. Solving the resulting LMI yields the state-feedback matrix  $K = 10^4 \times (-2.4784 - 1.5466 - 0.21082 - 0.0098271)$  having significantly smaller Euclidean norm  $2.9290 \times 10^4$  than in Section 4.1.

The initial position errors are zero while velocities errors are about 20%. For the sake of comparison, they are the same as in Section 4.1. The initial torque is much smaller now, yet still quite unrealistic for the actual model of Acrobot. Therefore, a saturation limit in the range  $\pm 10$  Nm was used, see Figure 5. In Figures 6 and 7 one can see the step trajectory

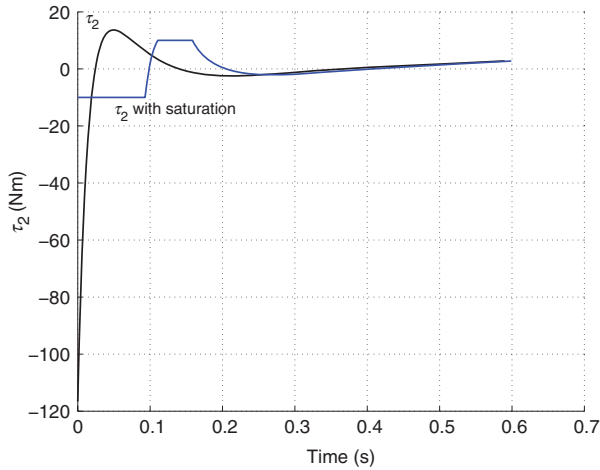


Figure 5. Torque  $\tau_2$  with and without saturation for prismatic bounds on  $\mu$ .

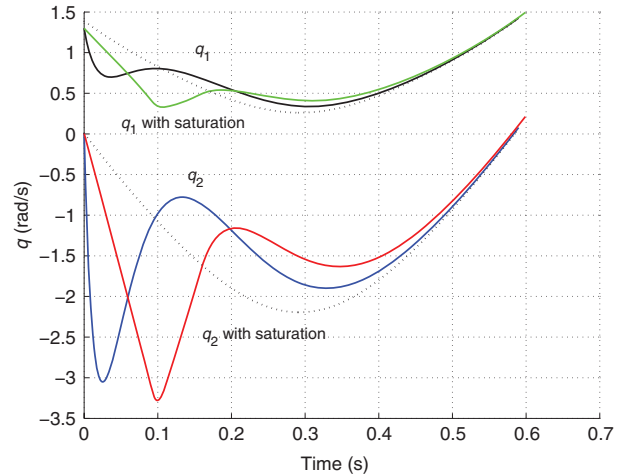


Figure 7. Angular velocities  $q_1, q_2$  with and without saturation and references (dotted line) for prismatic bounds on  $\mu$ .

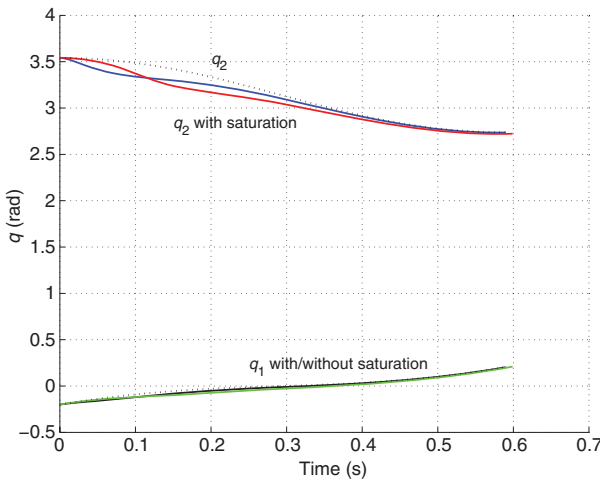


Figure 6. Angular positions  $q_1, q_2$  with and without saturation and references (dotted line) for prismatic bounds on  $\mu$ .

simulations with and without saturation limit. Convergence is very good now and saturation limits ensure a more realistic implementation. Moreover, though the saturated input torque time functions still quantitatively quite a lot differs from the non-saturated one, at least qualitative resemblance can be observed now.

### 4.3 $H_2$ design with box and prism

In order to further reduce the control effort, a complementary alternative to tighter uncertainty modelling consists in formulating the problem as a polytopic  $H_2$  design problem. In the standard state-space framework

$$\dot{x} = Ax + Bu + v, \quad z = Cx + Du,$$

with (fictitious) unit Gaussian white noise input  $v$  and (fictitious) performance output  $z$ , we aim at finding a static state feedback  $u = Kx$  minimising the energy functional

$$\lim_{T \rightarrow \infty} E \left[ \frac{1}{T} \int_0^T z^T z dt \right]. \quad (54)$$

In particular, setting

$$[C \mid D] = \begin{bmatrix} W_x^{1/2} & 0 \\ 0 & W_u^{1/2} \end{bmatrix}$$

for some given positive definite weighting matrices  $W_x$  and  $W_u$ , the integral term in quadratic objective function (54) becomes

$$\begin{aligned} \int_0^T z^T z dt &= \int_0^T (x^T W_x x + u^T W_u u) dt \\ &= \int_0^T x^T (W_x + K^T W_u K) x dt \end{aligned}$$

as in standard linear quadratic Gaussian (LQG) control.

In our context, choosing  $W_x = I_4$  and  $W_u = 1$  allows to penalise the control effort significantly, even though other values can be used to trade off. Using the standard Gramian interpretation of  $H_2$ -norm constraints, see e.g. Scherer and Weiland (2005, Section 4.3.3), an LMI formulation of static state-feedback design is as follows:

$$\begin{aligned} &\min_{Z, Q, Y} \text{trace } Z \\ &\text{s.t.} \quad \begin{bmatrix} Z & CQ + DY \\ (CQ + DY)^T & Q \end{bmatrix} \succeq 0 \\ &\quad A_i Q + B Y + (A_i Q + B Y)^T + I \leq 0, \quad i = 1, 2, \dots, \end{aligned}$$

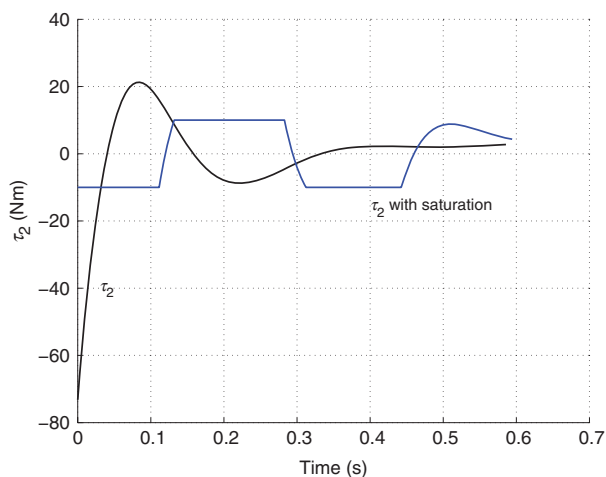


Figure 8. Torque  $\tau_2$  with and without saturation for the gains computed using 8-vertex rectangular box and  $H_2$  design.

where  $A_i$  ranges over vertices of the polytope containing the  $\mu(t)$  trajectory.

Using the 8-vertex rectangular box of Section 4.1 gives the state-feedback matrix  $K = 10^4 \times (-1.9301 - 0.97769 - 0.095525 - 0.0043721)$  with Euclidean norm  $2.1657 \times 10^4$  while the 6-vertex prism of Section 4.2 gives the state-feedback matrix  $K = 10^3 \times (-3.8704 - 2.3042 - 0.32191 - 0.025393)$  with the notably smaller Euclidean norm  $4.5159 \times 10^3$ .

To demonstrate the quality of the above designs in simulations, only the 8-vertex rectangular box is used. The simulations for the 6-vertex prism is quite similar to those of the Section 4.4 and are therefore omitted. The initial position and velocities errors are the same as before. Even if the initial torque is approximately 200 times smaller than the initial torque in the Section 4.1, still it is quite unrealistic for the Acrobot model. Again, the saturation limit in the range  $\pm 10$  Nm was used, see Figure 8. In Figures 9 and 10 one can see the effect of this saturation limit. Convergence is quite good now and even with saturations limiting the torques by the values  $\pm 10$  Nm it is possible to achieve exponential tracking. Nevertheless, the saturated torques time course is qualitatively different from the non-saturated one, which makes a more rigorous justification of convergence questionable.

#### 4.4 $H_2$ design with trajectory convex hull

As the last option, we choose to sample the trajectory at time instants  $t_i$ , and to let  $A_i = A(\mu(t_i))$  for  $i = 1, \dots, N$ . The corresponding uncertainty model is the polytopic convex hull of the  $A_i$  vertices. If we choose  $N = 279$  equidistant time instants, the resulting

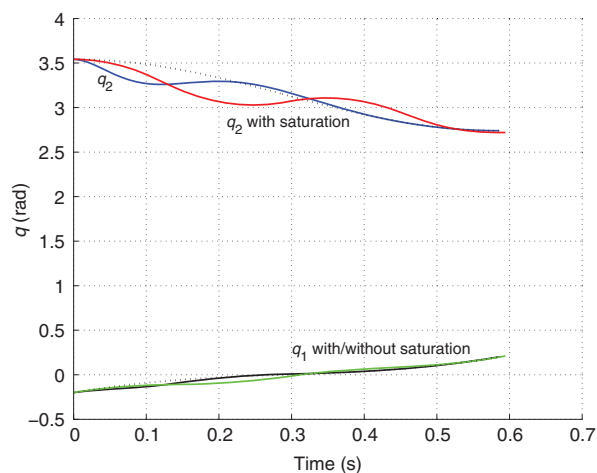


Figure 9. Angular positions  $q_1, q_2$  with and without saturation and references (dotted line) for the gains computed using 8-vertex rectangular box and  $H_2$  design.

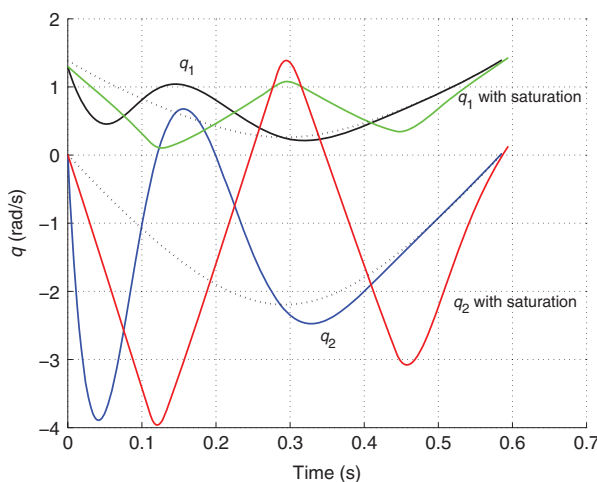


Figure 10. Angular velocities  $q_1, q_2$  with and without saturation and references (dotted line) for the gains computed using 8-vertex rectangular box and  $H_2$  design.

convex hull is a polytope with 274 vertices and 544 facets in the parameter space. Even though it is not guaranteed that the genuine trajectory  $\mu(t)$  is contained in this polytope, it is very close to the actual convex hull of the trajectory. The convex hull can be seen in Figure 11, note that it is interesting to compare it with prismatic bounds in Figure 4.

Solving the  $H_2$  design LMIs of Section 4.3, we obtain the state-feedback matrix  $K = 10^3 \times (-3.3407 - 2.0073 - 0.29683 - 0.024386)$  with Euclidean norm  $3.9087 \times 10^3$ . We observe that it is very similar to the matrix obtained with the  $H_2$  design with prismatic bounds. This is an indication that the manually designed polytope of Section 4.2 is a tight, yet simple approximation of the convex hull of the trajectory.

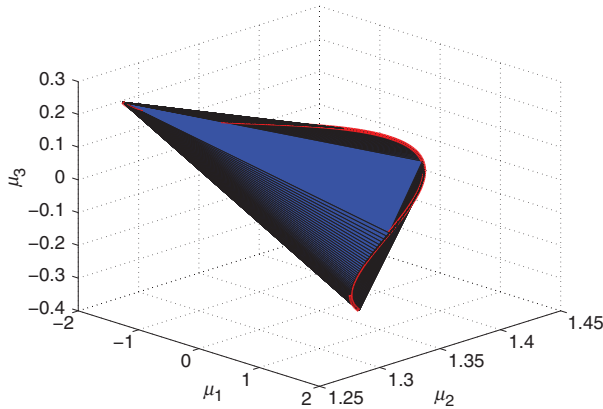


Figure 11. Trajectory  $\mu(t)$  and its convex hull.

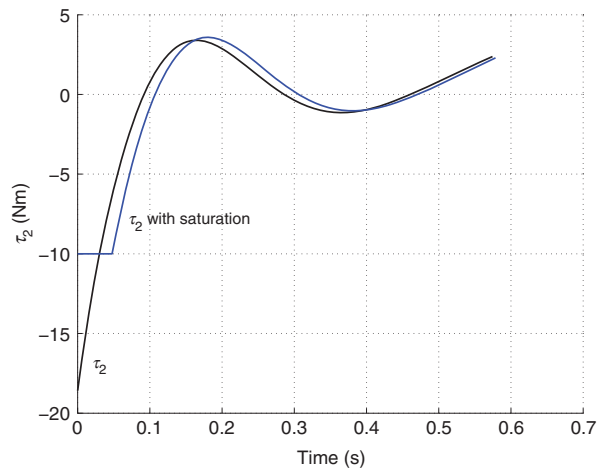


Figure 12. Torque  $\tau_2$  with and without saturation for the gains computed using the trajectory sampled convex hull and  $H_2$  design.

When using the above gains in tracking simulations, the initial position and velocities errors are the same as before. Although the initial torque is the smallest of all simulations, the saturation limit in the range  $\pm 10$  Nm was used, see Figure 12. The difference in simulation position and velocities with and without saturation limit is minimal, see Figures 13 and 14.

As the convergence is quite good now it is possible to use this feedback gain in realistic implementation. It is also very important that, unlike the saturations shown in Figure 8, the saturated torque Figure 12 is qualitatively very similar to the non-saturated one, thereby indicating possible more rigorous justification of the saturated stability.

**4.5 Summary of numerical results and tracking simulations**

The state-feedback gain matrices from Sections 4.1–4.4 are summarised in Table 1.

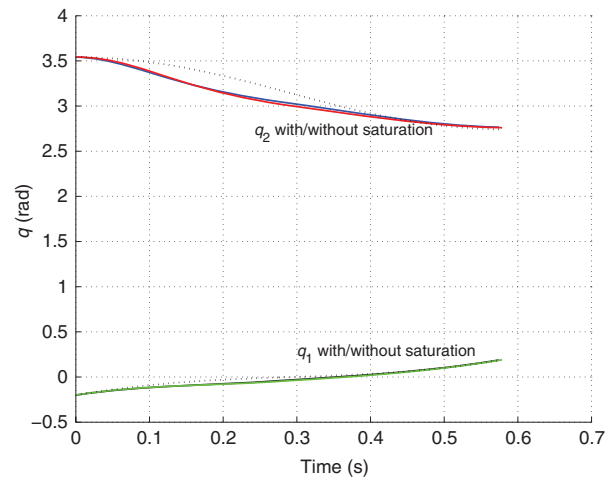


Figure 13. Angular positions  $q_1, q_2$  with and without saturation and references (dotted line) for the gains computed using the trajectory sampled convex hull and  $H_2$  design.

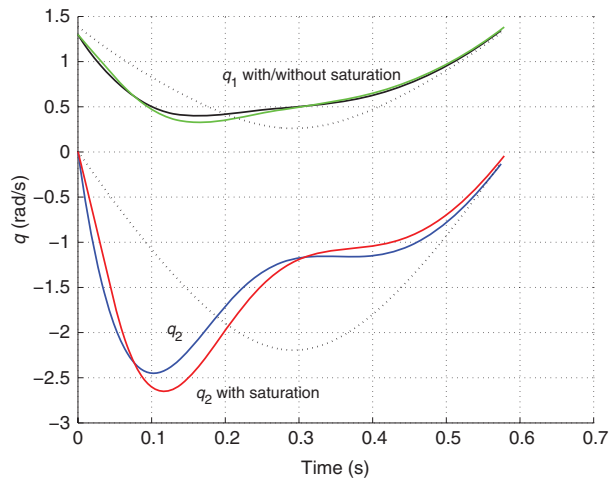


Figure 14. Angular velocities  $q_1, q_2$  with and without saturation and references (dotted line) for the gains computed using the trajectory sampled convex hull and  $H_2$  design.

Let us note that in the case of zero errors in initial position and velocities, almost any state-feedback gain matrix can be used, i.e. even with very low gains. As a consequence, very low torque is needed along the ideal target walking-like pseudo-passive trajectory. In other words, torques are mainly used to cope with deviation from the target trajectory. Nevertheless, in the case of the real Acrobot, the errors in initial position and velocities are always nonzero and the ability of reasonable high gains and resulting input torques has to be studied. In our analysis, the errors were typically less than 20%.

Table 1. Summary of the state-feedback gain matrices.

Method	State-feedback matrix $K$	Euclidean norm
Box	$10^5 \times (-1.9909 - 1.0082 - 0.10417 - 0.0020611)$	$2.2341 \times 10^5$
Prismatic	$10^4 \times (-2.4784 - 1.5466 - 0.21082 - 0.0098271)$	$2.9290 \times 10^4$
$H_2$ -box	$10^4 \times (-1.9301, -0.97769, -0.095525, -0.0043721)$	$2.1657 \times 10^4$
$H_2$ -prismatic	$10^3 \times (-3.8704, -2.3042, -0.32191, -0.025393)$	$4.5159 \times 10^3$
$H_2$ -sampling	$10^3 \times (-3.3407, -2.0073, -0.29683, -0.024386)$	$3.9087 \times 10^3$

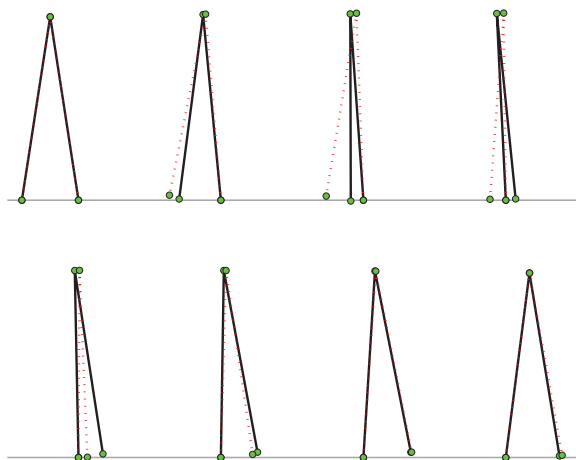


Figure 15. Animation of a single step with sampling time 0.08 s. The dotted line is the reference, the full line represents the actual Acrobot.

The design based on the rectangular box estimate without  $H_2$  optimisation is just able to track the walking trajectory but the lowest possible saturation limit is in the range  $\pm 25$  Nm and could not be further lowered. For this reason it is unacceptable in realistic implementation. Remaining designs of state-feedback gain matrix are able to track the walking trajectory with realistic saturation limits. Experimentally, the saturation in the range  $\pm 10$  Nm practically does not affect the quality of tracking, except the initial stage of the step. The design from Section 4.4 is able to track the walking-like trajectory with low and acceptable control effort.

Finally, to illustrate our approach more transparently, Figure 15 shows an animation of the Acrobot walking-like single-step trajectory with the state-feedback gain matrix from the last row of Table 1 and torque saturation of  $\pm 10$  Nm.

## 5. Conclusions and outlooks

An LMI-based design for stabilisation of error dynamics resulting from tracking a walking-like trajectory of the Acrobot has been suggested. Compared to earlier

analytic results in Čelikovský et al. (2008), Anderle et al. (2009) and Anderle and Čelikovský (2009), it gives now quite realistic torque at the Acrobot actuator.

Yet, further torque optimisation is possible via a further restriction of the set estimating parameter values. Namely, so far we have modelled the parameter trajectory as a polytope in the parameter space, and this allowed for the application of simple vertex LMI conditions corresponding to the search of a quadratic Lyapunov function. More sophisticated LMI conditions, based on representations of positive polynomials, can be derived for parameters varying along a curve, or within a general basic semialgebraic set (conjunction of multivariate polynomial inequalities). In the same vein, we could also derive LMI conditions to search for parameter-dependent polynomial-in-the-state Lyapunov functions, so as to reduce conservatism, if necessary.

Nevertheless, the issue of defining a criterion to minimise the input torque action remains open. We proposed  $H_2$  LMI design conditions to minimise the control effort, yet gains  $K$  affect real torques indirectly because of a nonlinear change of coordinates and feedback transformation between real torque  $\tau_2$  and virtual input  $w$ , resulting from partial exact feedback linearisation.

Regarding saturations of the control signal, we could also model them as sector-bounded nonlinearities and, as a post-processing phase, assess stability of the resulting closed-loop system in the presence of saturations via appropriate Lyapunov-based LMI conditions. These ideas are currently the subject of ongoing research.

## Note

1. Actually, by (2),  $\dot{\sigma} = \frac{d}{dt} \frac{\partial \mathcal{L}}{\partial q_1} = \frac{\partial \mathcal{L}}{\partial q_1}$  and therefore by (1),  $\dot{\sigma} = -\frac{\partial V(q)}{\partial q_1}$  as  $D(q) \equiv D(q_2)$  by (4). In other words,  $\dot{\sigma}$  has relative degree 2, i.e.  $\sigma$  has relative degree 3. Moreover, by straightforward differentiation it holds  $\dot{p} = d_{11}(q_2)^{-1} \dot{\sigma}$ , i.e.  $\dot{p}$  has relative degree 2, i.e.  $p$  should have relative degree 3 as well.

### Acknowledgements

We would like to thank Fabrizio Dabbene from Politecnico di Torino for fruitful discussion and useful tips. This research was supported by the Grant Agency of the Czech Republic through the grant no. 102/08/0186 and by Ministry of Education and Sports of the CR through the grant no. LA09026.

### References

- Anderle, M., and Čelikovský, S. (2009), 'Analytical Design of the Acrobot Exponential Tracking with Application to its Walking', in *IEEE International Conference on Control Automation (ICCA)*, Christchurch, New Zealand, pp. 163–168.
- Anderle, M., Čelikovský, S., Henrion, D., and Zikmund, J. (2009), 'LMI Based Design for the Acrobot Walking', in *IFAC Symposium on Robot Control (SYROCO)*, Gifu, Japan, pp. 595–600.
- Bortoff, S.A., and Spong, W.M. (1992), 'Pseudolinearisation of the Acrobot using Spline Functions', in *IEEE Conference Decision and Control (CDC)*, pp. 593–598.
- Čelikovský, S. (1994), 'Global Linearisation of Nonlinear Systems – A Survey', *Banach Center Publications*, 32, 123–137.
- Čelikovský, S., and Zikmund, J. (2007), 'Composite Control of the  $n$ -link Chained Mechanical System', in *Conference Process Control*, Vol. 130, Strbské Pleso, Slovakia, pp. 1–6.
- Čelikovský, S., Zikmund, J., and Moog, C. (2008), 'Partial Exact Linearisation Design for the Acrobot Walking', in *American Control Conference (ACC)*, Seattle, USA, pp. 874–879.
- Fantoni, I., and Lozano, R. (2002), *Non-linear Control for Underactuated Mechanical Systems*, Heidelberg: Springer Verlag.
- Furuta, K., Yamakita, M., and Kobayashi, S. (1991), 'Swing up Control of Inverted Pendulum', *Industrial Electronics, Control and Instrumentation*, 3, 2193–2198.
- Greiner, W. (2003), *Classical Mechanics: System of Particles and Hamiltonian Dynamics*, Berlin: Springer Verlag.
- Grizzle, J.W., Moog, C.H., and Chevallereau, C. (2005), 'Nonlinear Control of Mechanical Systems with an Unactuated Cyclic Variable', *IEEE Transactions on Automatic Control*, 50, 559–576.
- Hauser, J., and Murray, R.M. (1990), 'Nonlinear Controllers for Non-integrable Systems: the Acrobot Example', in *American Control Conference (ACC)*, San Diego, USA, pp. 669–671.
- Isidori, A. (1996), *Nonlinear Control Systems*, New York: Springer Verlag.
- Scherer, C.W., and Weiland, S. (2005), 'Linear Matrix Inequalities in Control', Lecture Notes, Delft University of Technology and Eindhoven University of Technology, The Netherlands, pp. 1–232.
- Spong, M. (1998), *Underactuated Mechanical Systems, Control Problems in Robotics and Automation*, London: Springer Verlag.
- Wiklund, M., Kristenson, A., and Åström, K.J. (1993), 'A New Strategy for Swinging up an Inverted Pendulum', in *IFAC World Congress*, Sydney, Australia, pp. 191–196.
- Zikmund, J., and Moog, C.H. (2006), 'The Structure of 2-Body Mechanical Systems', in *IEEE Conference on Decision and Control*, San Diego, USA, pp. 6464–6469.
- Zikmund, J., Čelikovský, S., and Moog, C.H. (2007), 'Nonlinear Control Design for the Acrobot', in *IFAC Symposium on Systems Structure Control (SSSC)*, Foz do Iguaçu, Brazil, pp. 1/6–6/6.